

ConDT: A 2D curve reconstruction algorithm based on a constrained-neighbor proximity graph

J. Antony · M. Reghunath · S. B. Thayyil · R. Muthuganapathy

1 **Abstract** We introduce ConDT algorithm, a proximity-
2 based reconstruction method relying on Delaunay Tri-
3 angulation. The underlying proximity graph is referred
4 to as the ConDT graph. In addition to being simple, the
5 algorithm could successfully handle various challenging
6 cases where classical reconstruction algorithms often
7 struggle. Outlier removal is done in the post-processing
8 phase using Interquartile Range (IQR) criteria, com-
9 puted for the specific instance of the proximity graph.
10 Relying on the recent benchmark on 2D reconstruction,
11 we show that our method works better or is on par with
12 the state-of-the-art methods.

13 **Keywords** Curve reconstruction · Delaunay triangula-
14 tion · epsilon sampling · outlier handling

15 1 Introduction

16 Given a planar point set $S \in \mathbb{R}^2$ where $S = \{v_1, \dots, v_n\}$
17 sampled from an unknown curve Σ , the goal is to ob-
18 tain “a piece-wise linear reconstruction of the curve”, C
19 from S that best approximates Σ . Curve reconstruction
20 has received significant attention in computational ge-
21 ometry and computer graphics over the past two decades.
22 Various algorithms [24] have been proposed to tackle
23 this problem under different assumptions and conditions.

J. Antony · M. Reghunath · R. Muthuganapathy
Advanced Geometric Computing Lab, Department of Engineering Design,
Indian Institute of Technology Madras, Chennai, India
E-mail: jomsantony@gmail.com, minureghunath@gmail.com, emry01@gmail.com
Corresponding author: J. Antony

Safeer Babu Thayyil
Department of Information Technology, Government Engineering College Palakkad, India
E-mail: safeerbabut@gmail.com

25 Many of the early curve reconstruction algorithms
26 assume that the input point set is sampled densely from
27 a simple, smooth curve. Some well-known classical algo-
28 rithms in this category include Crust, β -skeleton, NN-
29 Crust, and α -shapes. In general, an input point set may
30 exhibit characteristics such as non-uniform sampling,
31 noise, and outliers. Meanwhile, the resulting curves can
32 feature self-intersections, sharp corners, open ends, or
33 disconnected components. Classical algorithms that pro-
34 vide theoretical guarantees assuming ϵ -sampling, may
35 fail when the input point set contains the characteris-
36 tic(s) mentioned above.

37 To handle these, newer algorithms have often re-
38 sorted to tuning multiple parameters - a challenging
39 task in general. Algorithms that do not use any param-
40 eter or use only a single parameter have difficulties in
41 handling all the mentioned characteristics, as can be
42 seen from Table 1 in [24]. In particular, handling multi-
43 ple components, sharp corners, and outliers is challeng-
44 ing for such algorithms (refer to Table 1 in [24]).

45 Even the recent work [17] focuses only on manifold
46 curves on a clean point set and is unable to handle
47 outliers, open curves, curves with multiple components
48 and non-manifold curves. Self-intersection is a common
49 feature found in many planar curves. However, only a
50 few methods [13, 31, 27] address its reconstruction.

51 This work, tested on the publicly available bench-
52 mark [24], with the following contributions:

- 53 – Introduces ConDT graph - a basic proximity graph
54 structure which can be generated in a single-step
55 parallel procedure from DT(S).
- 56 – Algorithm is demonstrated to handle self-intersections,
57 multiple components, sharp corners (without any
58 parameters), and open curves (with a single param-
59 eter).

1 – Outliers are handled using a dynamically generated
 2 IQR parameter specific to the ConDT proximity
 3 graph.

4 2 Related work

5 Edelsbrunner proposed a Delaunay triangulation-based
 6 parametric method to produce α -shape [11], which char-
 7 acterizes the shape of a point set. Although it was not
 8 originally designed for curve reconstruction, its 3D ver-
 9 sion [11] was later shown to be applicable for this pur-
 10 pose.

11 Crust algorithms [1, 2] use a combination of De-
 12 launay triangulation and Voronoi diagram to produce
 13 closed/open curves. In Crust, a dense sampling based
 14 on medial axis transform was introduced by Amenta et
 15 al. [1], which is widely considered as a seminal work
 16 used to ensure theoretical guarantee of a reconstructed
 17 curve. Reconstruction using nearest neighbor graph with
 18 theoretical guarantee is presented in NN-Crust [7]. In
 19 Power Crust [2], a subset of Voronoi vertices known as
 20 poles is used to build a power diagram, which divides
 21 the plane into interior and exterior cells.

22 Noise filtering of a given point set and introducing
 23 new points, followed by pruning and reconstruction us-
 24 ing NN-Crust, is proposed by Cheng et al. [5]. Mehra
 25 et al. [18] proposed a visibility operator on the convex
 26 hull of a noisy point set and used the visibility informa-
 27 tion to perform both curve and surface reconstructions.
 28 Feiszli et al. [12] introduced a non-parametric deno-
 29 sing strategy for reconstructing a curve while preserving
 30 sharp corners. However, the three curve reconstruction
 31 algorithms mentioned above do not reconstruct open
 32 curves, disconnected components, or curves with self-
 33 intersections, and they are not designed to handle out-
 34 liers.

35 Lee [15] proposed a reconstruction method based
 36 on the moving least squares concept, specifically de-
 37 signed for noisy point sets to compute curves without
 38 self-intersections. Shape Hull [29] removes the edges of
 39 a Delaunay triangulation based on the position of the
 40 circumcenter of triangles to construct a simple closed
 41 divergent curve. Another Delaunay triangulation-based
 42 method, EC-Shape, uses the empty circle approach for
 43 outer boundary detection [20] and hole detection [19].
 44 EC-Shape can reconstruct non-divergent curves but not
 45 open curves.

46 The Water-Distribution-Model (WDM) Crust [29]
 47 is based on the Voronoi diagram and handles outliers.
 48 Crawl [28] reconstructs closed/open curves with dis-
 49 connected components and multiple holes; however, it
 50 does not handle noisy point sets. The Optimal Trans-
 51 port Cost method proposed by de Goes et al. [13] is

52 a greedy method designed to minimize the increase in
 53 transport cost for noisy point sets. Wang et al. [31] pro-
 54 posed a quad-tree method with smoothing concepts to
 55 reconstruct a curve from a noisy point set with out-
 56 liers. Most of the existing methods [10][29][20] are de-
 57 signed for simple closed curve reconstruction, whereas
 58 only a few of them [27][13][31] reconstruct both open
 59 and closed curves. A comprehensive survey and bench-
 60 marking of various algorithms for curve reconstruction
 61 are discussed by Ohrhallinger et al. [24]. This bench-
 62 mark includes about 15 reconstruction algorithms, in-
 63 cluding the recent ones. Recently, deep learning ap-
 64 proaches have also been explored for curve reconstruc-
 65 tion, where networks are trained to predict and fit uni-
 66 form B-splines to given point sets[4]

67 While several algorithms address aspects of curve
 68 reconstruction, it remains challenging to develop a gen-
 69 eralized algorithm that handles all features: closed/open
 70 curves, disconnected components, self-intersections, mul-
 71 tiple holes, and sharp corners, while also handling noise
 72 and outliers.

73 Although some reconstruction algorithms [20] [29][28]
 74 detect some of the mentioned features, they are not
 75 designed for handling noise. Algorithms specifically de-
 76 signed for handling noise [5] [18] [12] do not reconstruct
 77 open curves, disconnected components, or curves with
 78 self-intersections, and are not designed for handling out-
 79 liers. Lee [15] designed a reconstruction algorithm for
 80 noisy point sets for both closed and open curves, but
 81 it is not capable of detecting self-intersections. F. de
 82 Goes et al. [13] and Wang et al. [31] claim to handle
 83 noise, self-intersections, and outliers, but their results
 84 on clean input point sets are very poor. Additionally,
 85 many algorithms have multiple parameters, making it
 86 tedious to synchronize and tune them.

87 3 Overview

88 Key concepts with regard to curve reconstruction such
 89 as medial axis, local feature size, and ϵ -sampling are
 90 well established in the literature and can be found in
 91 the seminal work by Amenta et al[1]. A quick review
 92 of these concepts can be found in Section 1 of the Sup-
 93 plementary. Now we introduce ConDT, the proximity
 94 graph employed in our method.

95 3.1 ConDT Proximity Graph

96 A ConDT graph (Constrained Natural Neighborhood
 97 Delaunay Triangulation) is a subgraph of a Delaunay
 98 Triangulation (DT) of a point set, S . For each point p ,
 99 let $EN(p)$ denote the set of edges directly connected to

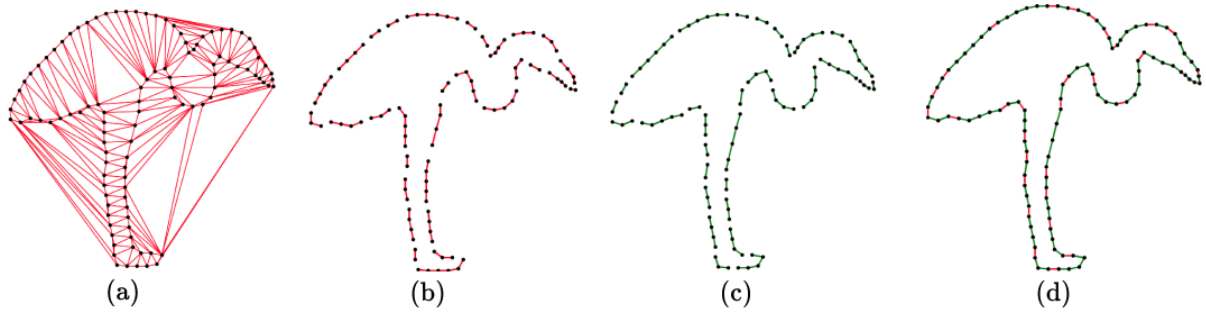


Fig. 1: Visualization of basic ConDT proximity graph construction (a) Input point set of bird and its DT (b) Shortest edge set say A from the natural neighbourhood of each point shown in red color (c) Second shortest edge set, say B in green color (d) Combining red and green edges to obtain our proximity graph ConDT which is $(A \cup B)$

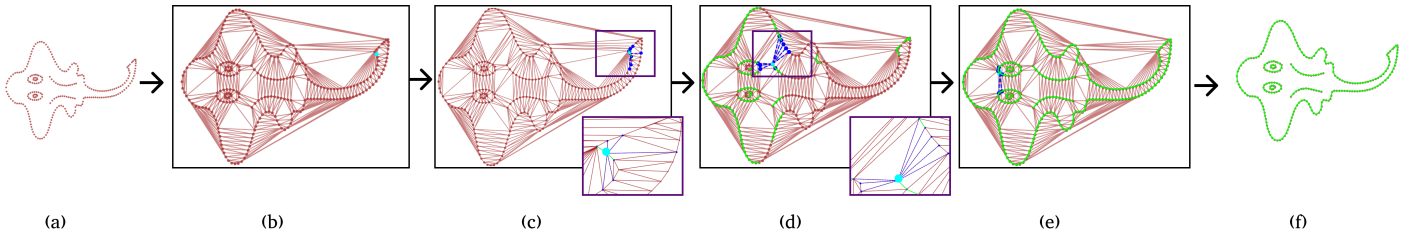


Fig. 2: Illustration of the proposed reconstruction algorithm on an input point set with multiple components and open curves in output. (a) Input point set (b) DT of the input point set (c) For an input point, p (in cyan), natural neighbours (shown in blue) with the selected edges (in green) (d) Illustration for a terminal point of an open curve (e) DT with reconstructed edges (in green) (f) Reconstructed output

¹ p in the DT, referred as natural neighborhood edges.
² ConDT graph is formed by retaining only the shortest
³ and second shortest edges from $EN(p)$ for each point
⁴ p , resulting in a simplified and filtered graph formally
⁵ defined as ConDT(S). This proximity graph produces
⁶ a valid reconstruction when the input point set is well-
⁷ sampled and free of outliers or noise.

⁸ Fig. 1 illustrates the construction of the ConDT graph.
⁹ Fig. 1 (a) shows an input point set representing
¹⁰ a bird shape adapted from the benchmark with addi-
¹¹ tional points to ensure sufficient sampling. The process
¹² involves selecting the shortest edge shown in red in Fig.
¹³ 1 (b) and the second shortest edge shown in green in
¹⁴ Fig. 1 (c) from the natural neighborhood of each point.
¹⁵ These selected edges are then combined into a set to
¹⁶ form the resulting ConDT proximity graph, as depicted
¹⁷ in Fig. 1 (d). This construction can be done in parallel
¹⁸ across all the input points.

neighborhood of each point p in the DT. From the set of edges in $EN(p)$, we retain only the first two shortest edges connected to each point to obtain ConDT(S). To take care of open curves (if any), one of the retained edges is to be removed based on a local uniformity parameter u . This parameter ensures the elimination of the longer edge by enforcing an allowable edge length ratio at each vertex.

The working of this algorithm is demonstrated with an example in Fig. 2. The input point set is shown in Fig. 2a along with its DT in Fig. 2b. For an input point p (in cyan), natural neighbourhood edges (in blue) and the selected edges (in green) are depicted in Fig. 2c. Illustration for another point is shown in Fig. 2d. in which only one green edge is selected, as the open curve criteria based on u parameter satisfies here. This basic reconstruction step is implemented in parallel for all points.

Instead of using a fixed value for u parameter, it can be adaptively computed on the go based on local neighbourhood as discussed in section 4.1

If reconstruction is limited to manifold curves, then we can handle non-manifold vertices in a post-processing

4 Method

The proposed method is outlined in the Algorithm 1. We start by constructing the DT of the input point set S . Identify the set of edges, $EN(p)$ in the natural

1 step (Line 11). This procedure is illustrated in Algorithm 2 and discussed in section 4.2.

2 Outlier removal is done (Line 12) as a post-processing
3 task and is illustrated in section 4.3.

Algorithm 1 ConDT(\mathbf{S})

Input: A planar point set $\mathbf{S} \subseteq \mathbb{R}^2$ representing the curve C , local uniformity parameter u .

Output: Reconstructed polygonal approximation, ∂O of the curve C .

```

1: Compute the 2D Delaunay triangulation,  $DT(\mathbf{S})$ .
2: for each point  $\mathbf{p}_i \in \mathbf{S}$  in parallel do
3:   Collect the set of 1-ring vertices,  $\mathcal{N}(\mathbf{p}_i)$ , incident to
    $\mathbf{p}_i$  in  $DT(\mathbf{S})$ .
4:   Collect the set of edges  $EN(\mathbf{p}_i)$  connecting  $\mathbf{p}_i$  to each
   of the vertices in  $\mathcal{N}(\mathbf{p}_i)$ .
5:   Retain the two shortest edges,  $e_1$  and  $e_2$ , in  $EN(\mathbf{p}_i)$ .
6:   if  $\max(e_1, e_2) \geq u \times \min(e_1, e_2)$  then
7:     Retain only the shortest edge,  $\min(e_1, e_2)$ , in
    $EN(\mathbf{p}_i)$ .
8:   Combine the retained edges in  $EN(\mathbf{p}_i)$  to form the edge
   set to obtain the proximity graph, ConDT( $\mathbf{S}$ ).
9: HANDLENONMANIFOLDS(ConDT( $\mathbf{S}$ ))
10: HANDLEOUTLIERS(ConDT( $\mathbf{S}$ ))

```

Algorithm 2 HandleNonManifolds

```

1: Input: Edge set ConDT( $\mathbf{S}$ ).
2: Output: Filtered edge set,  $filtEdges$ 
3: for each edge  $\{v_1, v_2\}$  in ConDT( $\mathbf{S}$ ) do
4:   if  $\text{degree}(v_1) \leq 2$  and  $\text{degree}(v_2) \leq 2$  then
5:     Push edge  $\{v_1, v_2\}$  to  $filtEdges$ 
6:   for each vertex  $v$  in ConDT( $\mathbf{S}$ ) do
7:     if  $\text{degree}(v) \geq 3$  then
8:       Push  $v$  to NonManifoldVertices
9:   for each vertex  $v$  in NonManifoldVertices do
10:    Find the shortest edge  $e_1$  from  $v$ 
11:    Find the edge  $e_2$  that gets the highest score based on
    angle and edge length criteria.
12:    Push  $e_1$  and  $e_2$  to  $filtEdges$ 
13: return  $filtEdges$ 

```

5 4.1 Adaptive computation of uniformity parameter u

6 Selecting u based on local sampling density or edge
7 length distributions allows the method to better accom-
8 modate variations in point spacing and curve structure.
9 In this section, we outline a strategy that uses local
10 neighbourhood information to compute the uniformity
11 parameter dynamically.

12 This strategy adapts u based on the local distribu-
13 tion of edge lengths in the 1-ring neighborhood of each
14 point, ensuring that edge comparisons remain propor-

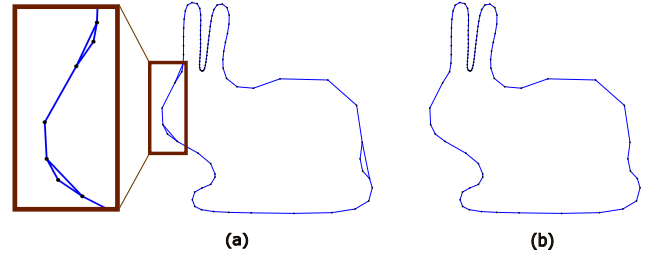


Fig. 3: (a) ConDT graph of a sparsely sampled input point set containing non-manifold vertices (some are shown in zoomed inset) (b) After removal of undesired edges using Algorithm 2

15 **ditional to the local scale. The adaptive computation is**
16 **performed as follows.**

17 For each point \mathbf{p}_i , we compute the set of edges in its
18 1-ring neighborhood, $EN(\mathbf{p}_i)$, and calculate the **mean**
19 edge length:

$$\ell_i = \text{mean}(\{\|e\| : e \in EN(\mathbf{p}_i)\})$$

20 The local threshold u_i is then computed as:

$$u_i = \frac{\ell_i}{\min(\|e_1\|, \|e_2\|)}$$

21 where e_1 and e_2 are the two shortest edges emanating
22 from \mathbf{p}_i . The edges are retained if:

$$\max(\|e_1\|, \|e_2\|) < u_i \cdot \min(\|e_1\|, \|e_2\|)$$

23 This strategy tunes the the parameter u to adapt
24 based on the local sampling density.

26 4.2 Handling Non-Manifold vertices

27 ConDT graph may end up with more than two edges
28 from the same vertex as shown in Fig. 3 a. We refer
29 to such vertices as non-manifold vertices. If we are
30 reconstructing simple closed manifold curves, no vertex
31 should have more than two edges attached to it. Non-
32 manifold handling involves the identification of non-
33 manifold vertices and retaining only the two most suit-
34 able edges. This is performed as a post-processing step
35 and is detailed in Algorithm 2. Here we iterate through
36 all non-manifold vertices and select at most two of them
37 based on certain criteria.

38 We always choose the first shortest edge as it is guar-
39 anteed to be present in the result following the ϵ - sam-
40 pling criteria in [7]. The second edge is chosen carefully
41 based on a scoring mechanism. The edge selection score
42 is given by

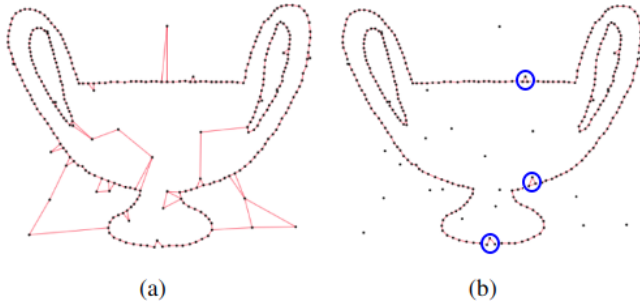


Fig. 4: (a) ConDT graph of input point set with outliers
(b) Removal of outlier edges using IQR criteria

$$\text{score} = \max_{\substack{e \in E \\ \theta_e > \frac{2\pi}{3}}} \left(\frac{\theta_e}{\pi} \times \frac{L_{\min}}{L_e} \right)$$

where:

- $\frac{\theta_e}{\pi}$ is the normalized angle at the vertex where edge e is incident.
- L_e is the length of edge e .
- L_{\min} is the shortest edge length among all candidate edges.

This score-based edge selection ensures the choice of an edge that forms a sufficiently large angle while favouring shorter edges for geometric consistency. The selection process enforces a minimum angle criterion of $\theta_e > \frac{2\pi}{3}$ to avoid choosing edges that are too sharp. We compute this score only for non-manifold vertices present in ConDT, unlike in NNCRUST [7] and HNNCRUST [21] where angle computation is done for every vertex. Fig. 3 illustrates how score-based selection helps in retaining only the suitable edges in the final output.

4.3 Handling Outliers

Algorithm 3 HandleOutliers

```

1: Let  $sqlengths$  be sorted list of squared edge lengths of ConDT(S).
2:  $Q1 = sqlengths[n/4]$ .
3:  $Q3 = sqlengths[3n/4]$ .
4:  $IQR = Q3 - Q1$ .
5:  $IQR_{th} = Q3 + 1.7 \times IQR$ .
6: for each vertex  $v_i \in \text{ConDT}(S)$  do
7:   if both outgoing edge lengths from  $v_i > 2.IQR_{th}$  then
8:     OUTLIERFOUND = true
9:     Break
10: if OUTLIERFOUND then
11:   Retain edges with squared lengths below the  $IQR_{th}$ .

```

Our proximity graph provides a good embedding of most of the retainable edges (part of the original curve) with some additional edges connected to the outlier points. Figure 4 (a) shows the ConDT graph of a point set containing outlier points.

The Interquartile Range (IQR) [14] method is used to filter out edges with unusually large lengths from the ConDT graph. The IQR threshold is computed from the sorted edge list. Edges with squared lengths below the computed IQR threshold are retained, effectively preserving edges that conform closely to the original shape, resulting in a better reconstruction as shown in Fig. 4b

This outlier removal is detailed in Algorithm 3. Testing various parameter values in the range [1.0, 3.0], we observed optimal results within the interval [1.7, 2.5], therefore we adopted 1.7 as the parameter value (refer to line 5 of Algorithm 3). Outlier points, generated using the benchmark implementation, include some placed very close to the curve, leading to a few undesired edges (see the regions enclosed in blue circle in Fig. 4b).

5 Results, Comparison & Discussion

We have tested and compared our method ConDT against 15 state-of-the-art curve reconstruction algorithms available in the benchmark implementation of “2D points curve reconstruction survey and benchmarking” [24] namely FITCONNECT [26], STRETCHDENOISE [25], CCRUST [8], PEEL [27], CRAWL [28], OPTIMAL-TRANSPORT [13], CONNECT2D [22], HNNCRUST [21], LENZ [16], CRUST [1], NNCRUST [7], GATHAN1 [9], GATHANG [6], DISCUR [32], VICUR [3] and also with the latest work SIGCONNECT [17]. For this we incorporated SIGCONNECT into the existing 2D Benchmark. OPTIMALTRANSPORT is omitted in some quantitative and qualitative evaluations, since it works only with input point sets with high level of noise and outliers and is unable to reconstruct clean point sets. We conducted a qualitative analysis by visually comparing the reconstructed curves, each exhibiting unique characteristics. For quantitative evaluation, we utilized metrics including exact reconstruction, RMS error, and runtime. The implementation is done using CGAL 5.6 [30] where parallel processing is enabled using Intel TBB (Threading Building Blocks) and tested on a system equipped with an Intel Core i7-12700 processor.

Table 1 shows the input and output capabilities of different algorithms along with their manifold guarantees, time complexity and capability of running on dense point set.

The results of ConDT on 3 different instances of simple closed curves, open curves, multiple curves, in-

Table 1: Comparison on input and output capabilities, time complexity, running times of various reconstruction algorithms. Under Input column notations used are **NU**: non uniform, **NO**: noisy, **OU**: outlier. The notations used under output column are **O**: open, **MU**: multiple components, **S**: sharp corners, **SI**: self intersections/non-manifold, **G**: guarantee. **T**: time complexity, **Exactness**: exact reconstruction

Algorithm	P	Input			Output					T	Dense Point Set	
		NU	NO	OU	O	MU	S	SI	G		Exactness	Run-time(ms)
FITCONNECT	0	yes	yes	yes	yes	yes	yes	no	yes	nk^2	yes	3503
STRETCHDENOISE	0	yes	yes	yes	yes	yes	yes	no	yes	nk^2	— Failed —	
CCRUST	0	yes	no	yes	yes	yes	no	no	yes	$n\log n$	yes	192
PEEL	2	yes	yes	yes	yes	yes	no	yes	yes	n^2	yes	749
CRAWL	0	yes	no	yes	yes	yes	no	no	no	$n\log n$	yes	34
OPTIMALTRANSPORT	0	yes	yes	yes	yes	yes	no	yes	yes	$n\log n$	no	222
CONNECT2D	0	yes	yes	no	no	no	yes	no	yes	$n\log n$	no	653
HNNCRUST	0	yes	no	no	yes	yes	no	no	yes	$n\log n$	yes	11
LENZ	2	yes	no	no	yes	no	yes	no	yes	$n\log n$	— Failed —	
CRUST	0	yes	no	no	no	yes	no	no	yes	$n\log n$	yes	10
NNCRUST	0	yes	no	no	yes	yes	no	no	yes	$n\log n$	no	4
GATHAN1	1	yes	no	no	yes	yes	yes	no	no	$n\log n$	yes	7
GATHANG	1	yes	no	no	yes	yes	yes	no	yes	$n\log n$	yes	78
DISCUR	0	yes	no	no	yes	yes	yes	no	yes	$n\log n$	— Failed —	
VICUR	4	yes	no	no	yes	yes	yes	no	no	$n\log n$	— Failed —	
SIGCONNECT	0	yes	no	no	no	no	yes	no	yes	$n\log n$	no	44
ConDT(Our's)	1	yes	no	yes	yes	yes	yes	yes	yes	$n\log n$	yes	6

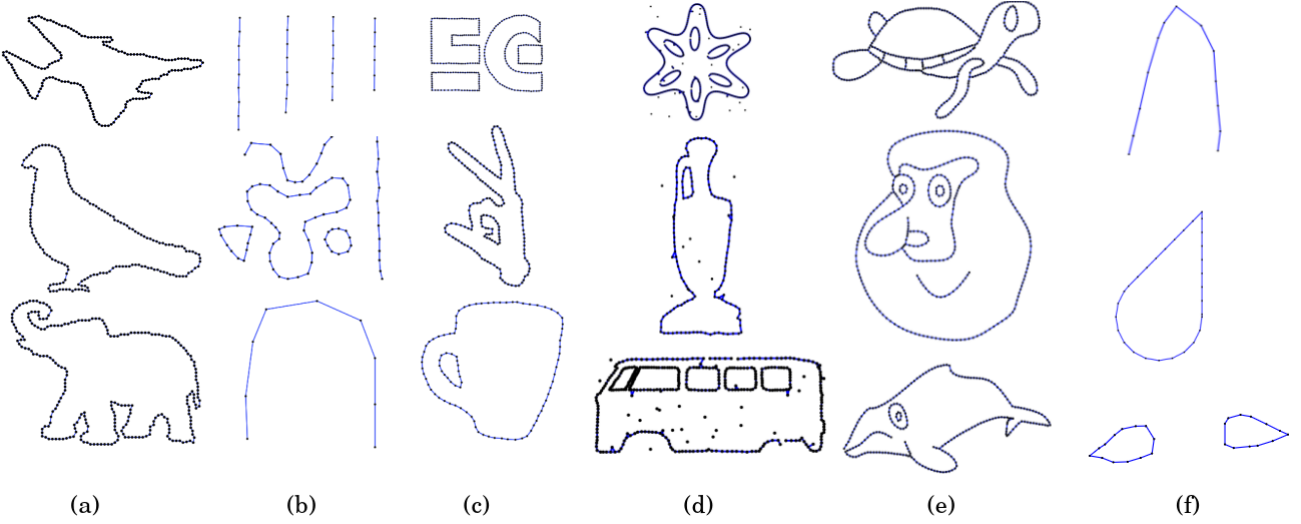


Fig. 5: Results obtained by ConDT on curves with different characteristics like (a) simple closed (b) open (c) multiple components (d) input with outliers (e) self intersections and (f) sharp corners.

1 put with outliers, curves with self-intersections, and
 2 curves with sharp corners are illustrated in Fig. 5.

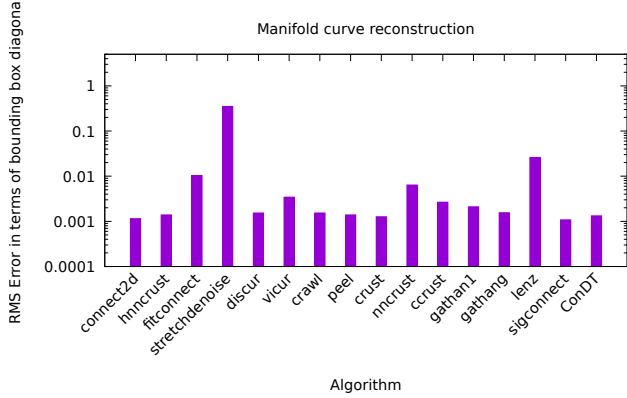


Fig. 6: RMS error of manifold curve reconstruction

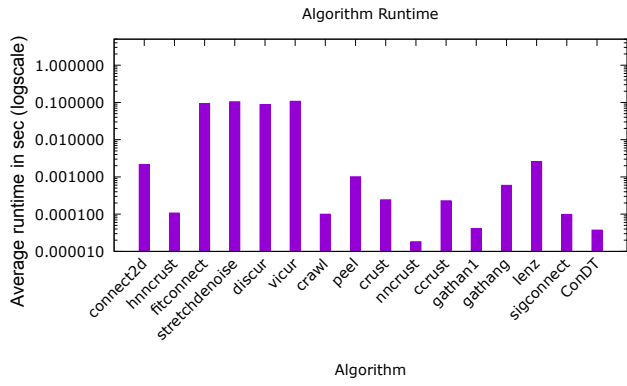


Fig. 7: Average runtime of manifold curves

3 **Manifold curves:** We selected a subset of 1,257
 4 noise-free point sets representing manifold curves from
 5 the original benchmark dataset for comparison. This
 6 subset is chosen in such way that the ones with all input
 7 points are interpolated in the ground truth is only
 8 included. Plots comparing RMS error is shown in Fig. 6.
 9 It can be noted that SIGCONNECT and CONNECT2D,
 10 which are optimized for manifold curve reconstruction,
 11 exhibited the minimum RMS error. However, they are
 12 not capable of reconstructing curves with other input
 13 and output features as indicated in table 1.

14 The plots in Fig. 6 show that ConDT is comparable
 15 to SIGCONNECT and CONNECT2D in terms of RMS error.
 16 The runtime plot in Fig. 7 illustrates that ConDT
 17 is on par with superior performers.

18 **Well sampled Manifold curves:** Sampling is ap-
 19 plied on a few simple closed curves - bunny shape from
 20 benchmark and blob and simple shapes from [23] to

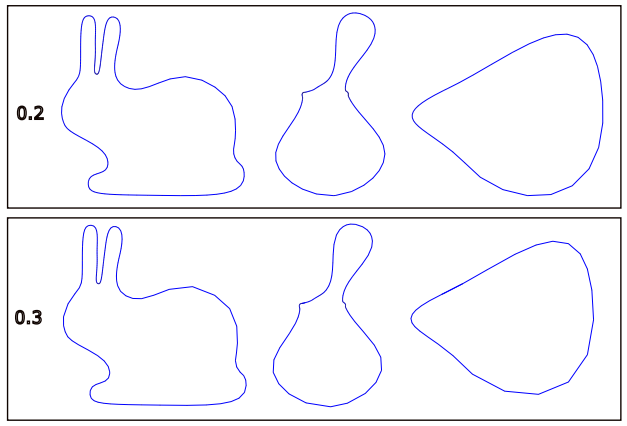


Fig. 8: Reconstruction of simple closed curves by ConDT with ϵ -sampling at $\epsilon=0.2$ and 0.3

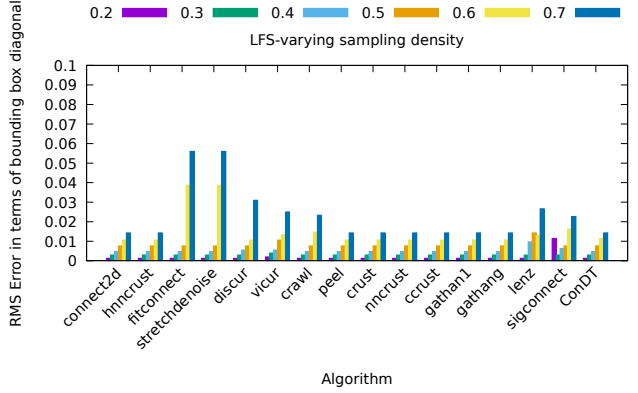


Fig. 9: RMS error of reconstruction for varying ϵ -sampling.

21 generate noise free point sets which follow the ϵ sampling
 22 criteria of $\epsilon = 0.2, 0.3, 0.4, 0.5, 0.6$, and 0.7 . Re-
 23 construction of 3 simple closed curves by ConDT with
 24 ϵ -sampling at $\epsilon=0.2$ and 0.3 is shown in Fig. 8. RMS error
 25 for reconstruction for varying ϵ sampling is shown in
 26 Fig. 9. CONDT is clearly superior against 7 algorithms
 27 and on par with other algorithms.

Densely sampled manifold curves:

28 Densely sampled point sets of over 10,000 points are
 29 obtained by sampling from the border samples available
 30 in the benchmark for testing.

31 The run-time and reconstruction exactness[24] of
 32 various algorithms are presented in Table 1. Despite
 33 the high sampling density, algorithms such as SIGCON-
 34 NNECT, CONNECT2D, NNCRUST, OPTIMALTRANSPORT,
 35 GATHAN and GATHANG failed to produce accurate re-
 36 construction. Furthermore, algorithms like STRETCH-
 37 DENOISE, LENZ, DISCUR, and VICUR were unable to
 38 generate the output. In contrast, our algorithm (a ba-

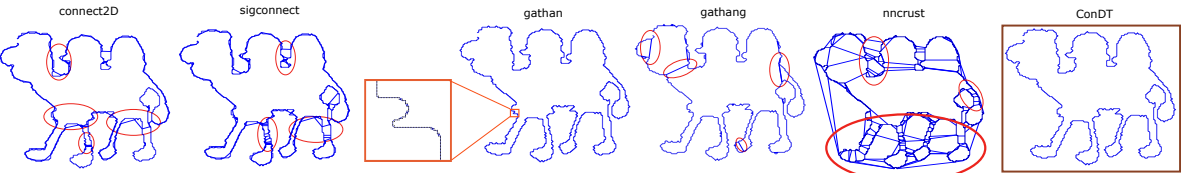


Fig. 10: Reconstruction on a densely sampled point set consisting of 10,518 points, our algorithm ConDT produced the exact reconstruction whilst algorithms like SIGCONNECT, GATHAN, GATHANG, NNCRUST generated incorrect results. (see the regions inside red ellipses) The Inset region for GATHAN shows break/incorrect connections.

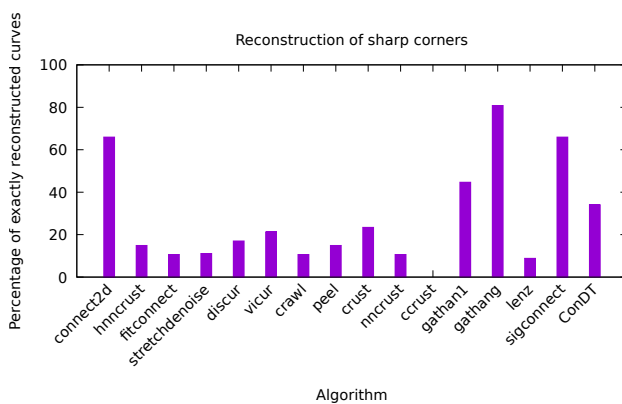


Fig. 11: Reconstruction of curves with sharp corners

sic version without non-manifold and outlier handling) successfully generated the correct output with a minimum runtime of 6ms. A qualitative comparison on a border sample representing the camel shape is shown in Fig. 10.

Sharp corners: We used 47 input point sets featuring sharp corners provided in the benchmark for comparison. The best results are obtained by GATHANG [6] and GATHAN [9] followed by CONNECT2D [22] and SIGCONNECT [17] (an improved version of CONNECT2D) which are specifically targeted at handling point sets with sparse sampling and sharp corners. Fig 11 presents the exactness plot, highlighting that while our algorithm is not specifically designed for sharp corners, it still achieved competitive performance, surpassing all the remaining algorithms.

Non-manifold/Self intersecting curves: Non-manifold /self-intersecting curves can be handled by our method (see Fig.1e). Fig. 12 presents the RMS error plot comparing different algorithms, demonstrating that ConDT performs competitively with the top performing methods.

Open and multiple curves: Our method is capable of handling open and multiple curves with sufficient sampling (see Fig.1b and Fig.1c). The reconstruction

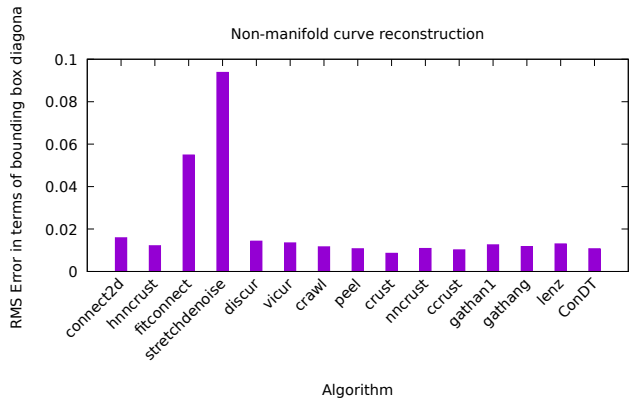


Fig. 12: Reconstruction of non-manifold/self-intersecting curves

for open curves can be fine-tuned by varying the local uniformity parameter u for each shape. Overall reconstruction exactness using a single parameter for all shapes is difficult to achieve. Here we used a common local uniformity parameter value, $u = 2.75$. However, we can evaluate the performance of different algorithms using a symmetric difference of area between the result obtained to the correct output[17]. This will help in validating that the reconstructed shapes closely resemble the expected output. The symmetric difference area (computed using BOOST's *boost_sym_diff*) between the output of different algorithms and the correct output is shown as a plot in Fig.13. It can be noted that the symmetric difference measure of ConDT is very low, second only to crust, which has the smallest value for open curves. RMS error comparison of different algorithms on multiple curves is shown in Fig. 14, it can be noted that the result is competitive with that of other algorithms.

We have also evaluated the performance of our method using an adaptively computed uniformity parameter, as described in Section 4.1. The comparative results using different algorithms with the adaptive uniformity parameter are provided in Section 2 of the Supplementary. The results are comparable to those obtained using a

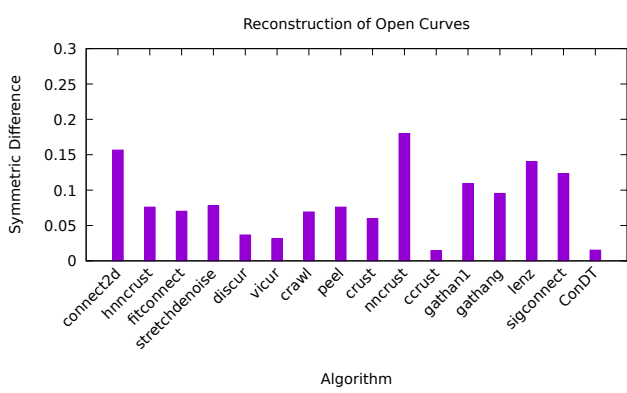


Fig. 13: Reconstruction of open-curves

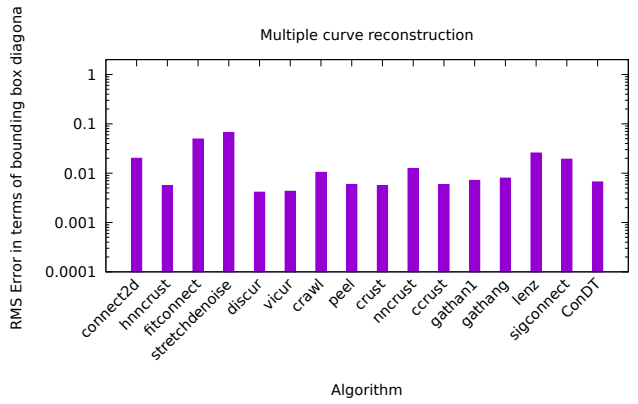


Fig. 14: RMS Error of reconstruction of multiple-curves

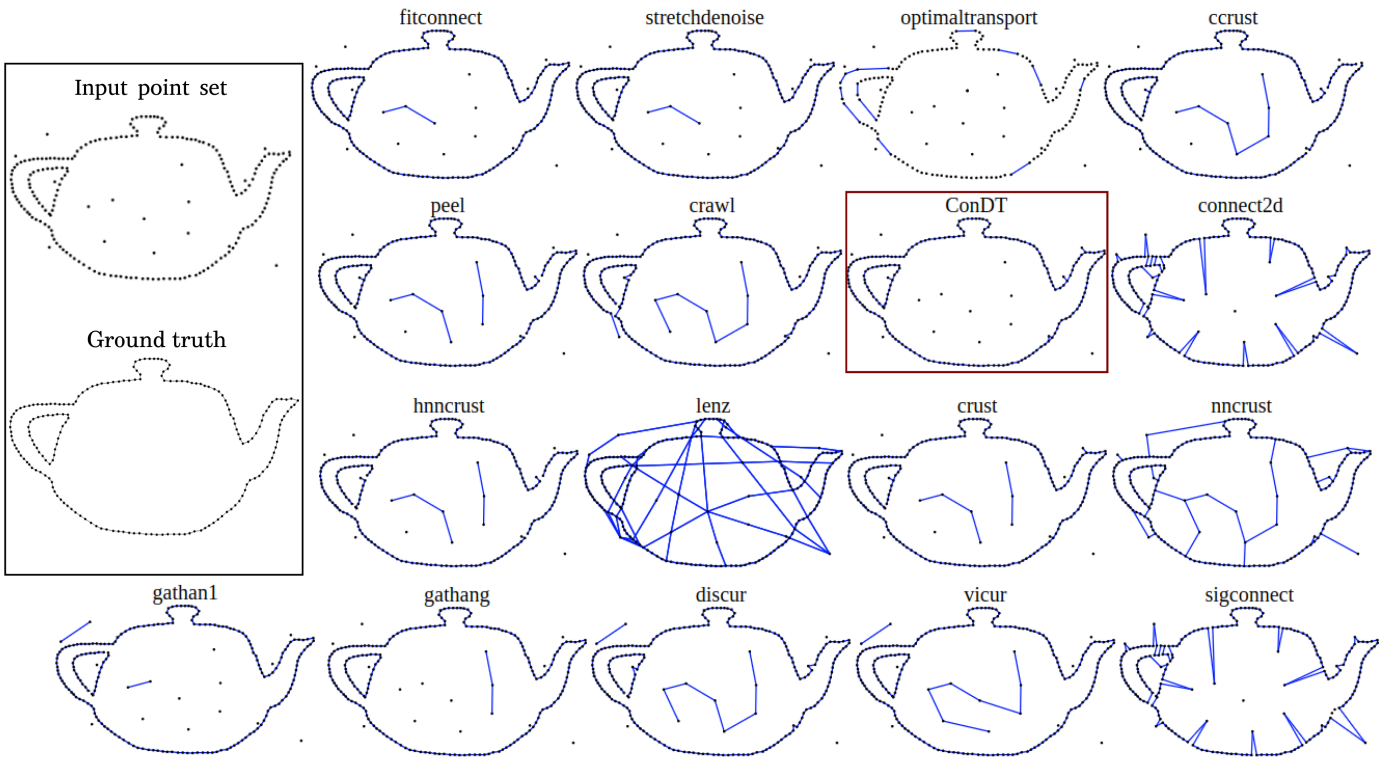


Fig. 15: Results of different curve reconstruction algorithms for input point set with 10% outliers. Input point set and ground truth is shown enclosed in black rectangle. ConDT result is enclosed in brown rectangle. Many long edges connected to outlier points are found in the output of other benchmark algorithms

1 carefully tuned u parameter. To fine tune the value u
 2 parameter, a sensitivity analysis is performed, RMS error
 3 is found to be minimum for u in range (2.5, 3.0).
 4 This plot is available in Section 2 of the Supplementary.

5 **Outliers:** Using the benchmark code[24], we evaluated
 6 our algorithm at different levels of outliers - 5%,
 7 10% and 20% and observed that it outperforms all the
 8 existing methods. Fig. 15 demonstrates the superior
 9 performance of ConDT in reconstructing input point
 10 sets containing outliers. Notably, other reconstruction

11 algorithms claiming to handle outliers either failed to
 12 remove many long edges (see results of FITCONNECT,
 13 STRETCHDENOISE, CCRUST, PEEL, CRAWL) or struggled
 14 to retain the desired edges (see OPTIMALTRANSPORT
 15 result). Algorithms like CONNECT2D, HNNCRUST,
 16 LENZ, CRUST, NNCRUST, GATHAN1, GATHANG, DISCUR,
 17 VICUR and SIGCONNECT do not have outlier handling
 18 capability, evident from the long undesirable edges in
 19 their reconstruction. Our algorithm has the minimum
 20 RMS error in all cases, as shown in Fig. 16. A value

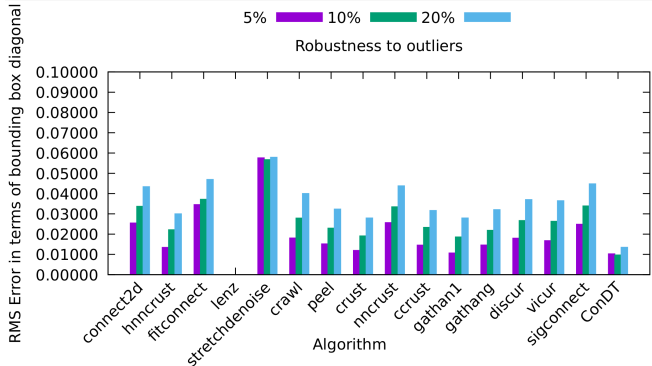


Fig. 16: RMS Error of reconstructed curves from the point set with 5%, 10% and 20% outliers added.

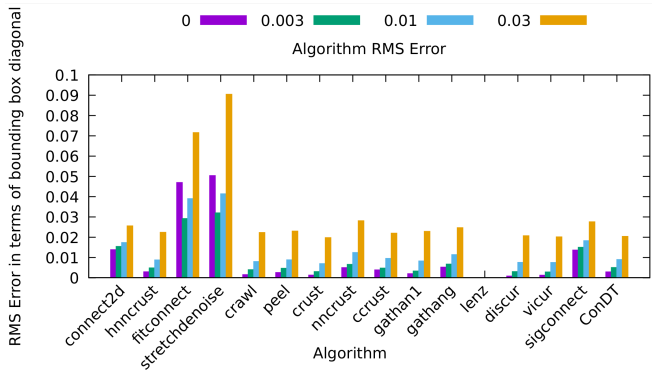


Fig. 17: RMS Error of reconstructed curves from the point set perturbed with uniform noise of $\delta = 0.003, 0.01$ and 0.03 as well as the non-noisy input.

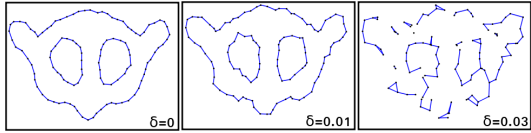


Fig. 18: Reconstructed curves with points perturbed with uniform noise of $\delta = 0$ (clean), 0.01 and 0.03 . CONDT managed to reconstruct the original shape with $\delta = 0.01$ but failed to recreate the shape at $\delta = 0.03$ similar to all other state-of-the-art algorithms.

¹ of 1.5 is generally chosen for IQR parameter as per statistics, but a sensitivity analysis for IQR parameter showed that a value of 1.7 is more appropriate. The sensitivity analysis plot for the IQR parameter is available in Section 2 of the Supplementary.

⁶ **Noise:** Robustness against noise is computed using the RMS error against the ground truth by introducing uniform noise levels of $\delta = 0.003, 0.01$ and 0.03 to the input curves. Here, noise level δ corresponds to the perturbation level with uniform noise as a percentage of the bounding box diagonal. The results are shown

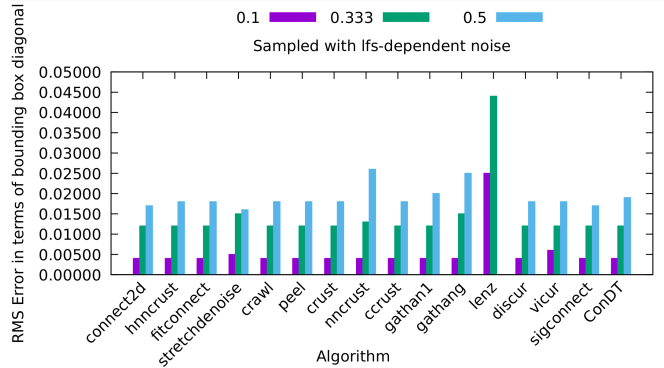


Fig. 19: RMS Error of reconstructed curves of points sampled with $\epsilon = 0.3$ and the points perturbed with local feature sized noise of $\delta = 0.1, 0.33$ and 0.5

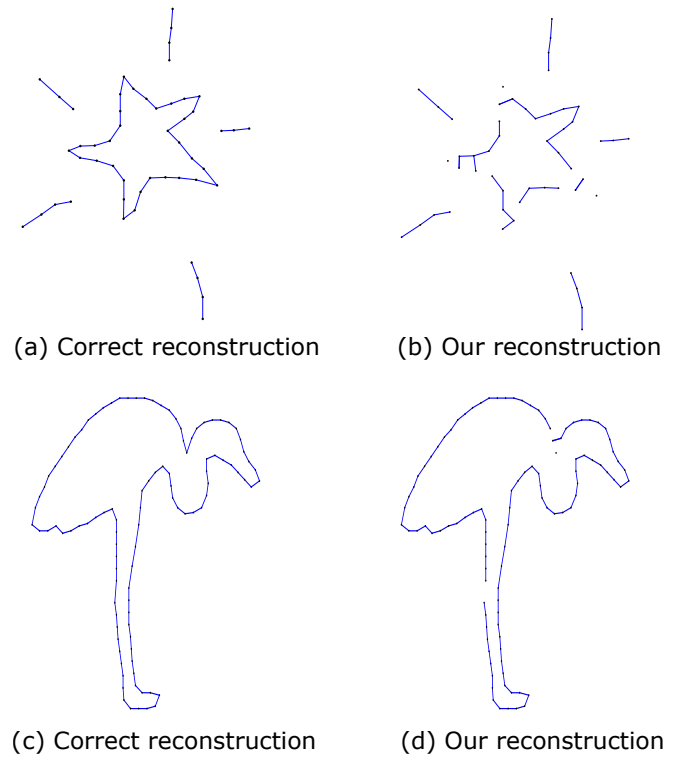


Fig. 20: A few failure cases

in Fig. 17. Our method CONDT exhibited the minimum RMS error in comparison with other state-of-the-art algorithms, even though our method is not explicitly designed for handling noise. Qualitative results for noise levels of 0 (noise-free), 0.01, and 0.03 for a curve with multiple components are illustrated in Fig. 18. Notably, CONDT managed to reconstruct the original shape with $\delta = 0.01$. For $\delta = 0.03$, our algorithm, as well as other state-of-the-art algorithms, failed to recreate the shape correctly. We also tested our method by

12
13
14
15
16
17
18
19
20
21

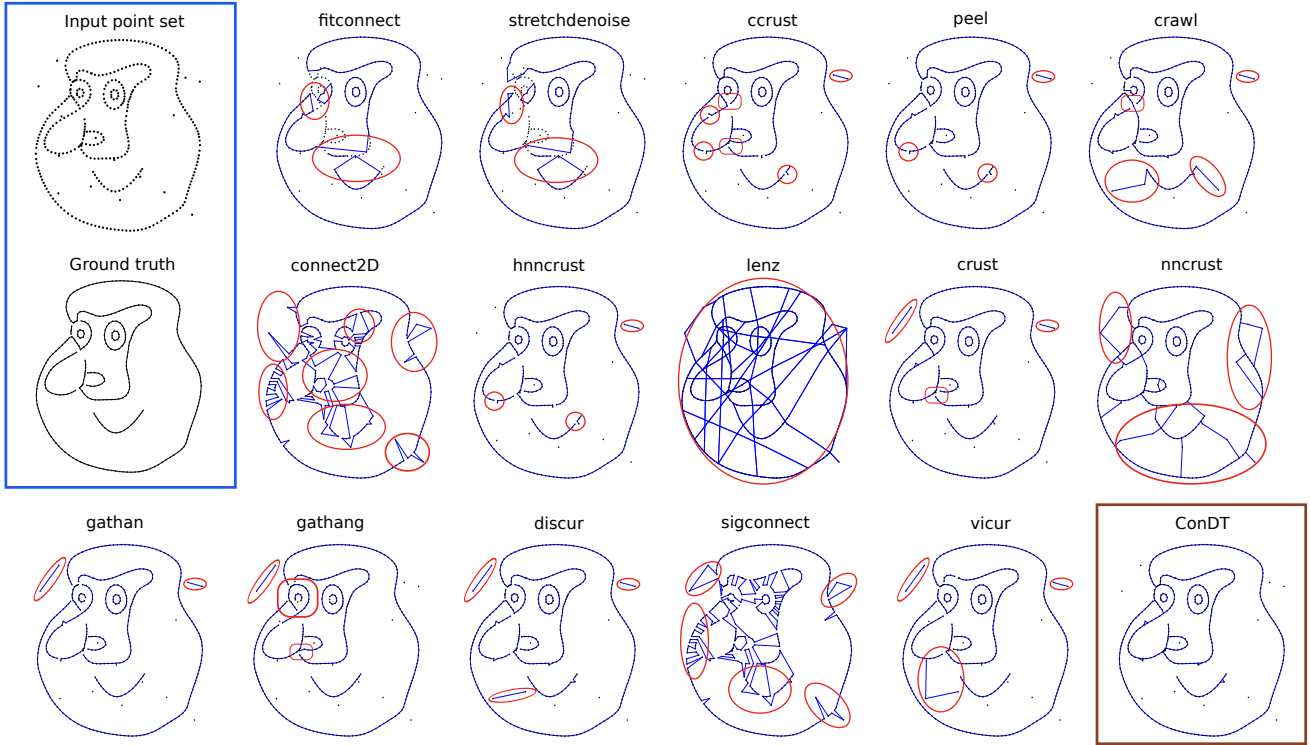


Fig. 21: Comparison of the results from different curve reconstruction algorithms applied to an input point set with various input characteristics, including (a) non-uniform sampling (b) presence of outliers (10%) and multiple output characteristics like (a) simple closed (b) open (c) multiple components or holes, (e) self-intersections. The input point set and ground truth are shown enclosed inside the blue rectangle. ConDT’s output is shown enclosed inside a brown square. Regions enclosed in red ellipses indicate incorrect edges, red circles show connection breaks and red rounded rectangles highlight incorrect self-intersections (for other algorithms).

1 adding lfs noise on samples along a cubic Bézier curve
 2 keeping $\epsilon = 0.3$; results for the same are depicted in
 3 Fig. 19, which are better or competitive with other al-
 4 gorithms.

6 Limitations

22 Our algorithm is not fine-tuned for handling noise, sharp
 23 corners, and sparse sampling. Although the current non-
 24 manifold and outlier handling approach works well in
 25 practice, it is not guaranteed to be error-free in all cases.
 26 Failure cases for outliers and noisy data are depicted in
 27 Fig. 4 (b) and Fig. 18 respectively. A few other failure
 28 cases are depicted in 20. Here (a) shows the correct re-
 29 construction of a curve with multiple components and
 30 open segments, while (b) shows our reconstruction. (c)
 31 is the correct reconstruction of a simple closed curve,
 32 and (d) shows our result. It can be noted that our
 33 results are affected by sparse sampling, non-manifold pro-
 34 cessing and parameter tuning. Another failure case oc-
 35 curs when two independent curves are sampled in close
 36 proximity. This scenario is illustrated in Section 2, Figure
 37 6 of the Supplementary material.

5 **Summary:** Unlike other state of the art algorithms,
 6 CONDT’s uniqueness is that it is capable handling vari-
 7 ous input characteristics like (a) non-uniform sampl-
 8 ing (b) presence of outliers, and multiple output char-
 9 acteristics like (a) simple closed (b) open (c) multi-
 10 ple components or holes, (e) self-intersections which is
 11 desirable in real use cases. The input point set depicted in Fig.
 12 21. is an example that embeds all the input and output
 13 features listed. It can be noted that the reconstruction
 14 result by CONDT is superior in comparison with other
 15 state-of-the-art algorithms. The reconstructed outputs
 16 of other algorithms exhibit one or more of the following
 17 defects: (a) retained connections to outlier points en-
 18 closed inside red ellipses, (b) incorrect self-intersections
 19 enclosed in red circles, and (c) breaks in connections
 20 enclosed within red rounded rectangles.

1 7 Conclusions and Future Work

2 We proposed a proximity graph-based reconstruction
 3 algorithm called CONDT. The CONDT proximity graph
 4 can be generated in a single parallelized step. The algo-
 5 rithm relies on a single parameter and is capable of re-
 6 constructing a wide range of characteristic curves. Our
 7 algorithm outperformed the state-of-the-art algorithms
 8 in outlier removal and noise handling in terms of RMS
 9 error. Moreover, it has exhibited superior performance
 10 in reconstructing highly dense point clouds in terms
 11 of exactness and runtime, as well as when multiple in-
 12 put and output features are present. In future work,
 13 CONDT can be further enhanced to explicitly address
 14 noisy input point sets and **locally non-uniform sampling**
 15 (e.g., regions with $\epsilon > 1$). Moreover, it can be extended
 16 to 3D for parallel surface reconstruction.

17 References

- 1 Amenta, N., Bern, M., Eppstein, D.: The crust and
 2 the beta-skeleton: Combinatorial curve reconstruction.
 3 Graphical Models and Image Processing pp. 125–135
 4 (1998)
- 5 Amenta, N., Choi, S., Kolluri, R.K.: The power crust.
 6 In: Proceedings of the Sixth ACM Symposium on Solid
 7 Modeling and Applications, SMA '01, pp. 249–266. ACM
 8 (2001)
- 9 An Nguyen, T., Zeng, Y.: Vicur: A human-vision-
 10 based algorithm for curve reconstruction. Robotics
 11 and Computer-Integrated Manufacturing **24**(6), 824–834
 12 (2008). FAIM 2007
- 13 Barzegar Khalilsaraei, S., Komar, A., Zheng, J., et al.: In-
 14 ceptcurves: Curve reconstruction using an inception net-
 15 work. The Visual Computer **40**, 4805–4815 (2024)
- 16 Cheng, S.W., Funke, S., Golin, M., Kumar, P., Poon,
 17 S.H., Ramos, E.: Curve reconstruction from noisy sam-
 18 ples. Computational Geometry **31**(1), 63–100 (2005)
- 19 Dey, T., Wenger, R.: Fast reconstruction of curves with
 20 sharp corners. Int. J. Comput. Geometry Appl. **12**, 353–
 21 400 (2002)
- 22 Dey, T.K., Kumar, P.: A simple provable algorithm for
 23 curve reconstruction. In: SODA '99, pp. 893–894 (1999)
- 24 Dey, T.K., Mehlhorn, K., Ramos, E.A.: Curve reconstruc-
 25 tion: Connecting dots with good reason. Computational
 26 Geometry **15**(4), 229–244 (2000)
- 27 Dey, T.K., Wenger, R.: Reconstructing curves with sharp
 28 corners. Computational Geometry **19**(2), 89–99 (2001). Combinatorial Curves and Surfaces
- 29 Duckham, M., Kulik, L., Worboys, M.F., Galton, A.: Effi-
 30 cient generation of simple polygons for characterizing the
 31 shape of a set of points in the plane. Pattern Recognition
 32 **41**(10), 3224–3236 (2008)
- 33 Edelsbrunner, H., Mücke, E.P.: Three-dimensional alpha
 34 shapes. ACM Transactions on Graphics **13**(1), 43–72
 35 (1994)
- 36 Feiszli, M., Jones, P.W.: Curve denoising by multiscale
 37 singularity detection and geometric shrinkage. Applied
 38 and Computational Harmonic Analysis **31**(3), 392–409
 39 (2011)
- 40 de Goes, F., Cohen-Steiner, D., Alliez, P., Desbrun, M.: An
 41 optimal transport approach to robust reconstruction
 42 and simplification of 2d shapes. Computer Graphics Forum
 43 (2011)
- 44 Han, J., Kamber, M., Pei, J.: 2 - getting to know your
 45 data. In: J. Han, M. Kamber, J. Pei (eds.) Data Mining
 46 (Third Edition), The Morgan Kaufmann Series in Data
 47 Management Systems, third edition edn., pp. 39–82. Morgan
 48 Kaufmann, Boston (2012)
- 49 Lee, I.K.: Curve reconstruction from unorganized points.
 50 Computer-Aided Geometric Design **17**(2), 161–177
 51 (2000)
- 52 Lenz, T.: How to sample and reconstruct curves with
 53 unusual features. In: Proceedings of the 22nd European
 54 Workshop on Computational Geometry (EWCG), pp. 3,
 55 8, 12, 16, 20. Delphi, Greece (2006)
- 56 Marin, D., Ohrhallinger, S., Wimmer, M.: SIGDT: 2D
 57 curve reconstruction. Computer Graphics Forum **41**(7),
 58 25–36 (2022)
- 59 Mehra, R., Tripathi, P., Sheffer, A., Mitra, N.J.: Visibil-
 60 ity of noisy point cloud data. Computers and Graphics
 61 (2010). In Press, Accepted Manuscript
- 62 Methirumangalath, S., Kannan, S.S., Parakkat, A.D.,
 63 Muthuganapathy, R.: Hole detection in a planar point
 64 set: An empty disk approach. Computers & Graphics
 65 **66**, 124–134 (2017)
- 66 Methirumangalath, S., Parakkat, A.D., Muthuganapathy,
 67 R.: A unified approach towards reconstruction of a
 68 planar point set. Computers & Graphics **51**, 90–97 (2015)
- 69 Ohrhallinger, S., Mitchell, S., Wimmer, M.: Curve recon-
 70 struction with many fewer samples. Computer Graphics
 71 Forum **35**(5), 167–176 (2016)
- 72 Ohrhallinger, S., Mudur, S.: An efficient algorithm for de-
 73 termining an aesthetic shape connecting unorganized 2d
 74 points. Computer Graphics Forum **32**(8), 72–88 (2013)
- 75 Ohrhallinger, S., Parakkat, A.D., Memari, P.: Feature-
 76 Sized Sampling for Vector Line Art. In: Pacific Graphics
 77 Short Papers and Posters. The Eurographics Association
 78 (2023)
- 79 Ohrhallinger, S., Peethambaran, J., Parakkat, A., Dey,
 80 T., Muthuganapathy, R.: 2D points curve reconstruction
 81 survey and benchmark. Computer Graphics Forum **40**,
 82 611–632 (2021)
- 83 Ohrhallinger, S., Wimmer, M.: Stretchdenoise: paramet-
 84 ric curve reconstruction with guarantees by separating
 85 connectivity from residual uncertainty of samples. In:
 86 Proceedings of the 26th Pacific Conference on Computer
 87 Graphics and Applications: Short Papers, PG '18, p. 1–4.
 88 Eurographics Association, Goslar, DEU (2018)
- 89 Ohrhallinger, S., Wimmer, M.: Fitconnect: Connecting
 90 noisy 2d samples by fitted neighbourhoods. Computer
 91 Graphics Forum **38**(1), 126–137 (2019)
- 92 Parakkat, A.D., Methirumangalath, S., Muthuganapathy,
 93 R.: Peeling the longest: A simple generalized curve
 94 reconstruction algorithm. Computers & Graphics **74**,
 95 191–201 (2018)
- 96 Parakkat, A.D., Muthuganapathy, R.: Crawl through
 97 neighbors: A simple curve reconstruction algorithm.
 98 Computer Graphics Forum (2016)
- 99 Peethambaran, J., Muthuganapathy, R.: A non-
 100 parametric approach to shape reconstruction from
 101 planar point sets through delaunay filtering. Computer-
 102 Aided Design **62**, 164–175 (2015)
- 103 The CGAL Project: CGAL User and Reference Manual,
 104 5.6 edn. CGAL Editorial Board (2023). URL <https://doc.cgal.org/5.6/Manual/packages.html>

- 1 31. Wang, J., Yu, Z., Zhang, W., Wei, M., Tan, C., Dai,
2 N., Wei, L.: Robust reconstruction of 2d curves from
3 scattered noisy point data. Computer-Aided Design **50**
4 (2014)
- 5 32. Zeng, Y., Nguyen, T.A., Yan, B., Li, S.: A distance-
6 based parameter free algorithm for curve reconstruction.
7 Computer-Aided Design **40**(2), 210–222 (2008)